Detrapping and diffusion of H and D implanted in carbon studied by high temperature laser annealing and depth profiling

F. Schiettekatte, G.G. Ross *, B. Terreault

INRS-Énergie et Matériaux, 1650 Boulevard Lionel-Boulet, Varennes, Qué., Canada J3X 1S2

Abstract

The depth profiles of H and D implanted at low energy (0.7 and 1.5 keV) in Highly Oriented Pyrolytic Graphite (HOPG) (*a*-axis) and vitreous carbon (v-C), and then partially released by pulsed laser induced desorption were investigated in order to understand the H behaviour in carbon at high temperature. During the laser desorption experiment, the re-emitted gas quantity was measured as a function of laser energy density by mass spectrometry. Depth profiles of H and D remaining after partial desorption were also obtained by means of the elastic recoil detection (ERD)-$\mathbf{E} \times \mathbf{B}$ technique. Firstly, a significant difference between the re-emitted H_2 or D_2 gas quantity and the released amount deduced from the ERD profiles is observed. This could be explained by atomic H release or by far in-depth diffusion of molecules. Secondly, it is seen from the depth profiles of hydrogen in HOPG that no profile modification is observed below 1500 K. The desorption process is compatible with a local molecular recombination model with fast diffusion of the molecules. At higher temperatures, significant diffusion of atomic hydrogen allows it to be retrapped in the vacancy profile created during the implantation. © 1998 Elsevier Science B.V. All rights reserved.

1. Introduction

Carbon materials have been studied for many years as candidates for plasma-facing components in magnetic confinement fusion devices. The graphite, for example, has excellent thermal characteristics such as thermal conductivity, heat capacity, sublimation and outgassing temperatures. However, its affinity for hydrogen and other gases results in problems of contamination, of recycling coefficient determination and of in-vessel tritium inventory [1]. Carbon also displays complex sputtering behaviour and radiation enhanced sublimation [2,3]. While beryllium may also be used as plasma-facing material, graphite is still widely used in many tokamaks.

Therefore, it is necessary to understand the behaviour of the implanted hydrogen in graphite for a better understanding of the problems mentioned above. Many investigations have been conducted to measure the detrapping and diffusion coefficients, often by means of thermal desorption spectrometry. They show widely scattered values of the diffusion parameters. Ashida and Watanabe [4] proposed that the compensation effect (i.e. material structure dependence of the diffusion paths) should be responsible for the scatter in the diffusion data. The pre-exponential factor appears to be correlated to the activation energy when the different diffusion coefficient data are compared.

According to Sawicki et al. [5], depth profiling of implanted tritium showed no significant depth profile shape modification up to 1600 K. This is consistent with local molecular recombination with rapid diffusion of the molecules to the surface. No shift or widening of the tritium depth distribution is measured, which would be observed if a diffusion limited process was taking place. As a matter of fact, depth profile modification

---

* Corresponding author. Tel.: +1-514 929 8108; fax: +1-514 929 8102; e-mail: ross@inrs-ener.uquebec.ca.

studies prove to be a more effective tool to identify the mechanisms responsible for the desorption.

Most of the works on the hydrogen re-emission from carbon were conducted by means of classical thermal desorption. However, our group has studied the thermal release of hydrogen from a variety of carbon materials [6,7] by means of laser flash induced desorption [8,9]. This method is more or less analogous to isochronal annealing with very short time stages ($\sim 10^{-7}$ s) reaching elevated temperatures (>2000 K for carbon materials). The desorption parameters are deduced from the measured quantity of gas desorbed during each laser shot (of increasing energy density). This is achieved by a simulation of the desorbed quantities by means of the computer program DTRLAS [10], in which the coefficients of different desorption mechanisms are adjustable. Nevertheless, although it requires more complicated procedures, the measurement of the depth profile modification by a high depth-resolution and quantitative technique should allow a better understanding of the effective processes at high temperature, as mentioned above for classical thermal desorption.

This article investigates the depth profile modification by laser flash desorption of hydrogen and deuterium implanted in Highly Oriented Pyrolytic Graphite (HOPG) and vitreous carbon (v-C). These materials have been chosen for their contrasting structures (highly crystalline and nearly amorphous, respectively). It will be possible to find out if the processes at high temperature can be described by the same processes/parameters as those found at lower temperatures.

2. Experimental

Guo et al. [6] studied the laser induced re-emission of deuterium along the c-axis in HOPG (Union Carbide). In our study, HOPG samples used were cut parallel to c-axis. The main impurity is 2% H. No annealing was done in order to avoid any change in the materials structure. Both v-C and HOPG samples were polished with 3 μm diamond suspension followed by 0.04 μm alumina suspension finish. They were implanted at room temperature with 0.8 and 1.5 keV hydrogen and deuterium at fluences ranging from 2.5×10^{20} to 13.5×10^{20} at/m^2.

The samples were transferred in air from the implantation chamber to the laser desorption setup where the base pressure was maintained below 1×10^{-8} Torr by means of ion pump and cryogenic trap. A laser desorption experiment in our laboratory usually consists of a ramp of successive laser shots of increasing energy density (0.02–2.0 × 10^4 J/m^2) on the same spot. A Q-switch ruby laser was used ($\lambda = 694$ nm, 30 ns FWHM Gaussian shaped pulse). The H or D pressures were measured accurately by a quadrupole mass spectrometer (QMS) during the milliseconds following the laser pulse. The QMS was calibrated by means of calibrated H$_2$ and D$_2$ leaks with an accuracy of 6%. The HD (mass 3) was taken into account in the measurement of both H and D. In the present experiment, in order to minimize the accumulation of small effects and facilitate the comparison between the simulated and measured H and D distributions, the depth profile modification measurements were made on samples that had been subjected to a single laser flash.

The depth profiling was achieved by means of the elastic recoil detection analysis (ERDA) [11] with a filter consisting of crossed electric and magnetic fields in place of the absorber foil. This technique is called ERD-$\mathbf{E} \times \mathbf{B}$ [12]. In this technique, the depth resolution is not degraded by straggling in an absorber. The 350 keV ^{4}He beam ions are close to their stopping power maximum. This improves the depth resolution as well, which is approximately 3 nm at the surface for carbon. However, in order to achieve sufficient particle separation, the filter entrance must be tightly collimated, reducing as well the solid angle. A new $\mathbf{E} \times \mathbf{B}$ filter was installed [13] closer to the sample holder in order to maximize the solid angle ($\Delta \Omega = 2.06 \times 10^{-5}$ sr), which is 10 times larger than the solid angle of the original setup. The beam is incident at 25° angle relatively to the surface of the sample, while the detection angle is 45°. The beam spot size on target is 1.0 mm^2. A low beam fluence of 7.7×10^{19} He/m^2 was used in order to avoid any significant beam induced desorption [14]. The energy spectra are converted to quantitative depth profiles by means of the computer program ALEGRIA [15]. The depth profiles presented here are still resolution broadened.

Such profiles obtained on as-implanted samples are used as initial profiles in DTRLAS simulations. In short, DTRLAS calculates by finite differences the photon absorption and heat flow as a function of time and depth. In addition, the H or D evolution is calculated by simulating the detrapping and diffusion processes. The calculations last until the material temperature has cooled down. Surface molecular recombination and Soret effect can also be calculated but they have not been considered here because there is no evidence that these effects are important here (e.g. atomic hydrogen accumulation at surface).

3. Results

Fig. 1 shows the results of laser induced desorption experiments conducted on the samples for which H or D depth profile modification will be presented in this section. The symbols connected by lines represent the cumulative quantity of hydrogen desorbed as H$_2$ or D$_2$ molecules and measured by mass spectrometry after each laser shot of increasing energy. The symbols inside circles represent the loss of H or D as measured by
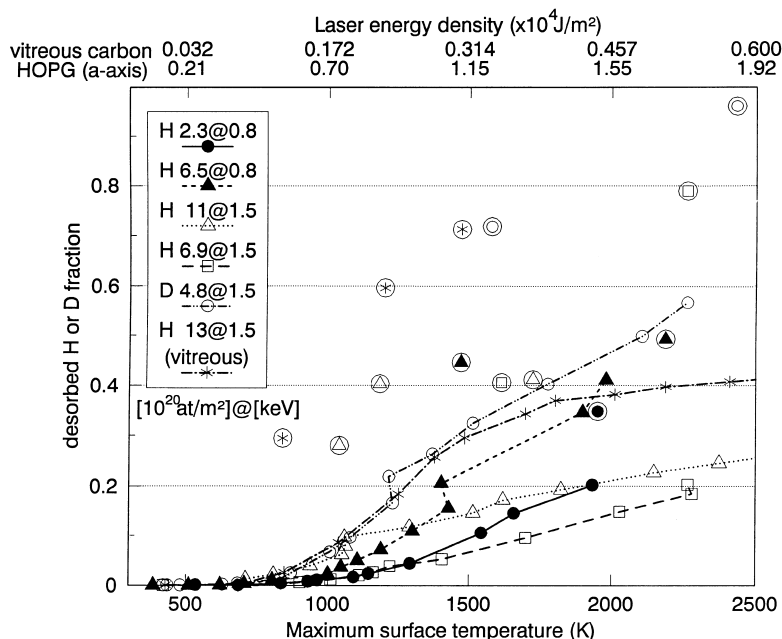
Fig. 1. Cumulative fractions of H_2 or D_2 desorbed as measured by a mass spectrometer (line + symbol) after laser shots of increasing energy density. Also shown are the H or D fraction lost from the implanted region as measured by ERD-$E \times B$ (symbols in circle) after a single laser shot. The implanted species and its implantation dose and energy appear in legend. Open symbols represent 1.5 keV H or D implantation in HOPG (*a*-axis) while closed symbols represent 0.8 keV H implantations. Symbol * is for H in vitreous carbon.

ERD-$E \times B$ (depth profile integral) after a single laser shot. These quantities were normalised to the implanted amount. The implanted species and its implantation dose and energy appear in legend. The lower horizontal axis represents the maximum temperature reached by the surface of the sample for each laser flash, as calculated by DTRLAS, according to the measured incident energy density. The corresponding energy density scales also appear on the upper axis. One can see that the energy density required to reach a given temperature is more than 3 times larger for HOPG than for v-C. This is due to the high thermal conductivity of graphite along the *a*-axis compared to *c*-axis or to isotropic carbon materials. The accuracy of the temperature/energy density is mainly influenced by the uncertainty on the evaluation of the laser spot size (±4%), while the accuracy of the amount of desorbed particles is dependent on the uncertainty on the pressure-to-quantity conversion factor (±6%). For clarity purposes, no error bars were included in Fig. 1.

For the v-C sample, the maximum energy density of 1.7×10^4 J/m² allowed to reach a maximum surface temperature of 5000 K, according to the computer code. The final cumulative desorbed H fraction is ~0.5 at that temperature. Similar temperature was reached for the HOPG sample implanted with 1.5 keV H. To do so, the laser was focused to reduce the spot surface by a factor of 3. However, the desorbed surface becomes so

small (0.9 mm² instead of 2.7 mm²) that no depth profiling measurements can be done. The final cumulative released H fraction was 0.35, but significant surface degradation of the sample was observed, such as increase of surface roughness and appearance of elongated cracks parallel to the crystal plane a^b. One can see in Fig. 1 that the loss measured by ERD is systematically greater than that measured by mass spectrometry. The physical significance of this difference will be discussed below.

At this point, the possibility of laser induced ablation of carbon samples is worth discussing. It is obvious that for lower temperatures ($T < 2500$ K), as those used in Fig. 1, no carbon ablation is expected, nor is it observed either by scanning electron microscopy (SEM) or by a shift in the depth profiles. In fact, no carbon ablation was observed even at higher temperatures (2500 K $< T <$ 5000 K), although some ablation could conceivably have occurred above the sublimation temperature (3925 K). Consequently, there is no impact on the depth profiles (unchanged within error bars), and there are no vapour/plasma shielding effects on the surface temperature. Some surface roughness was observed only on one HOPG sample heated up to 5000 K (as mentioned in the previous paragraph) for which no ERD measurement was performed.

The depth profiles are presented in Figs. 2–5. Fig. 2 shows the depth profile modification of H implanted at 0.8 keV in HOPG. The initial H contents are (a)
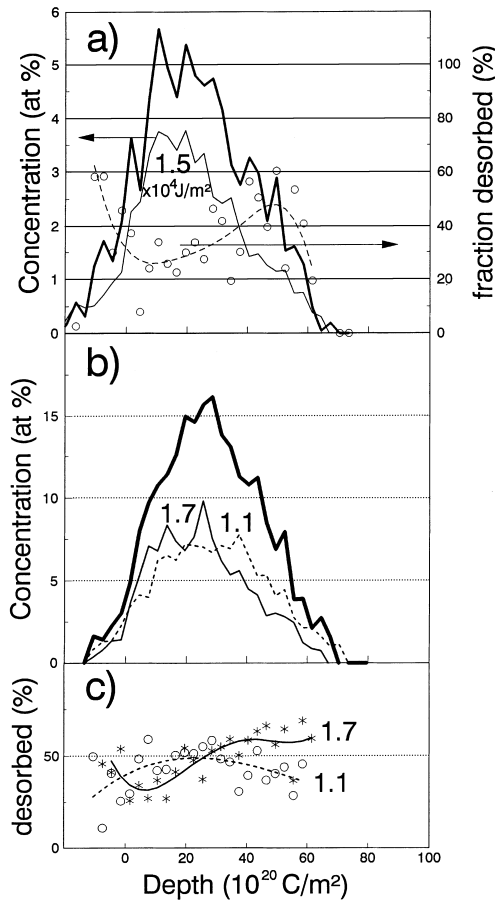
Fig. 2. (a) Depth profile modification of 2.3×10^{20} H/m² implanted at 0.8 keV in HOPG; depth profiles are shown as implanted (▬▬) and after a laser shot. The number on the curves represent the laser energy density. The lost H fraction also appears ($- \ominus -$). (b) 6.5×10^{20} H/m² were implanted; the implanted depth profile (▬▬) appears with those following laser flashes (numbers represent laser energy densities). (c) Lost fraction profiles corresponding to H depth profiles in (b).

2.3×10^{20} H/m² and (b) 6.5×10^{20} H/m², respectively. The depth profile integrals show that 35% of the hydrogen is lost after a laser shot of 1.5×10^4 J/m² in (a), while in (b) 45% and 49% are lost after laser shots of 1.1×10^4 and 1.7×10^4 J/m², respectively. Given $C(x)$ the H concentration as a function of depth, the lost fraction

$$Y(x) = \frac{C(x)_{\text{initial}} - C(x)_{\text{retained}}}{C(x)_{\text{initial}}} \qquad (1)$$

is also plotted together with the depth profiles in Fig. 2(a) while the desorbed fractions corresponding to the depth profiles in Fig. 2(b) appear in Fig. 2(c).

H or D was implanted at 1.5 keV in the four other samples. In Fig. 3(a), the initial H quantity is 11×10^{20} H/m². Three single laser shots depleted 28% (0.7×10^4
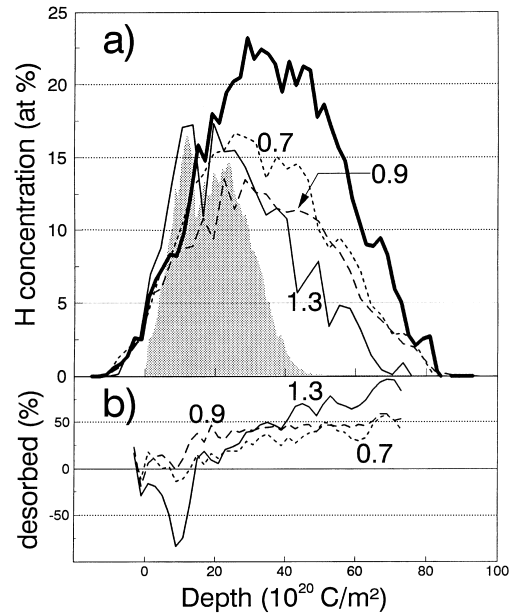

Fig. 3. (a) Depth profile modification of 11×10^{20} H/m² implanted at 1.5 keV in HOPG; depth profiles are shown as-implanted (▬▬) and after laser shots of indicated energies; the shaded region represents the vacancy profile. (b) Corresponding lost fractions.

J/m²), 40% (0.9×10^4 J/m²) and 41% (1.3×10^4 J/m²) of the hydrogen profiles, respectively. The corresponding lost fractions are plotted in Fig. 3(b). In Fig. 4(a), the initial H amount is 6.9×10^{20} H/m² of which 41% and 79% depleted after 1.2×10^4 and 1.7×10^4 J/m² laser shots while in Fig. 4(b) 4.8×10^{20} D/m² was implanted of which 72% and 96% desorbed after laser shots of 1.2×10^4 and 1.9×10^4 J/m², respectively. The *intrinsic* H profile after 1.9×10^4 J/m² is also shown. Finally, Fig. 5 shows the depth profile modification of 13×10^{20} H/m² implanted in v-C. Once again, three single laser shot depleted 29% (0.13×10^4 J/m²), 60% (0.23×10^4 J/m²) and 71% (0.31×10^4 J/m²) of the implanted hydrogen, respectively. Corresponding lost fractions appear in Fig. 5(b).

4. Discussion

4.1. Detrapping energy

At first glance, it is seen in Fig. 1 that, in HOPG, the hydrogen (●,▲,△,□) desorbs more slowly than the deuterium (○). One could think that the H is trapped with a higher binding energy. However, this is physically doubtful. Moreover, different detrapping energies would influence the temperature threshold where the desorption starts to take off. Because this is not observed, all
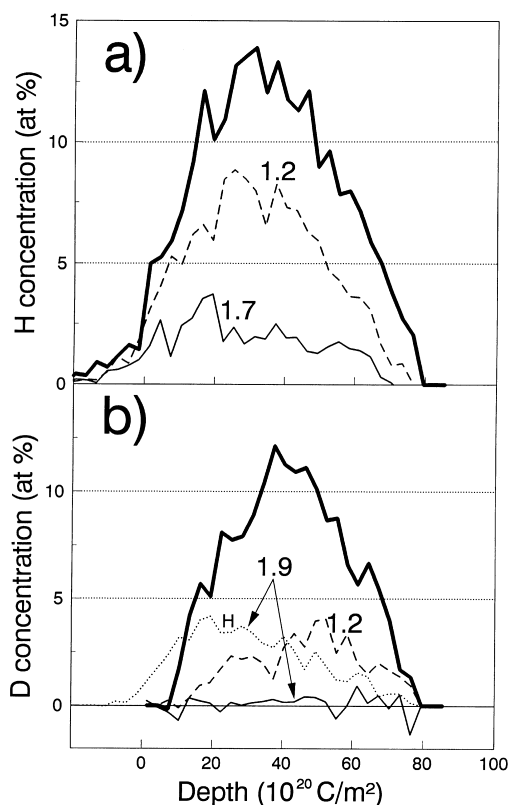
Fig. 4. (a) Depth profile modification of 6.9×10^{20} H/m² implanted at 1.5 keV in HOPG; depth profiles are shown as-implanted (▬▬) and after laser shots of indicated energies. (b) deuterium was implanted to a fluence of 4.8×10^{20} D/m²; the implanted depth profile (▬▬) appears with those following laser flashes of indicated energies. Also shown is the H depth profile in the same sample, resulting from intrinsic H retrapping after the 1.9×10^4 J/m² laser flash.

the data should correspond to the same detrapping energy. In order to calculate this energy, the initial H depth profile of Fig. 3(a) was put in DTRLAS in order to simulate the corresponding desorption curve of Fig. 1. Both the detrapping energy and the diffusion coefficient parameters were adjusted to give the best fit. The detrapping energy is found to be 0.6 eV, as obtained earlier by Kéroack and Terreault [7] for the same material and the same crystal orientation.

4.2. Differences in desorbed quantities

It is seen in Fig. 1 that the quantity of hydrogen desorbed as H_2 or D_2 (as measured by mass spectrometry) is a factor of 2–4 smaller than the depleted quantity found by the profiling method. One expects similar desorbed quantities in both cases and, moreover, the fi-
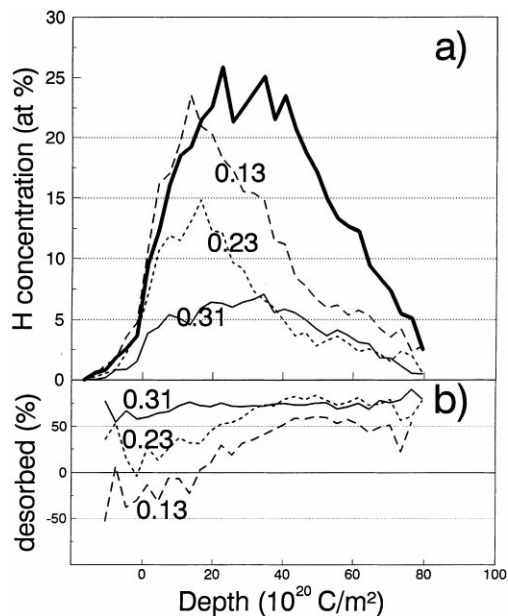

Fig. 5. (a) Depth profile modification of 13×10^{20} H/m² implanted at 1.5 keV in vitreous carbon; depth profiles are shown as implanted (▬▬) and after laser shots of indicated energies. (b) Corresponding desorbed fractions.

nal cumulative fraction desorbed as H_2 or D_2 should be close to 100%, as it is observed in other materials such as beryllium and silicon [6,16].

Kéroack and Terreault [7] showed that during laser induced desorption of D from carbon, a significant D amount formed HD molecules, while an equivalent quantity remained *undetected*. Also the intrinsic hydrogen concentration in carbon was not sufficient to account for all the H-D molecular recombination. These authors therefore suggested that *atomic* D desorption occurred, with some D–H recombination in the vacuum chamber, presumably on its inner walls. Atomic D desorption has also been evidenced by Franzen et al. [17], Franzen and Vietzke [18] and Davis and Haasz [19] at temperatures above 1500°C, a fact which strengthens the assumption of atomic desorption. Unfortunately, the atomic D (mass 2) could not be observed in the present experiment because the mass spectrometer was not directly aligned with the target and atomic D and H_2 have the same mass. The D desorbed as CD_4 (or other hydrocarbons) contributed only for a small part of the total D amount.

For the HOPG implanted with deuterium, the factor between the measured D_2 ($- \ominus -$ in Fig. 1) and the D actually lost as measured by ERD-$\mathbf{E} \times \mathbf{B}$ (⊚) is comparable to the difference found by Kéroack and Terreault. In the case of hydrogen implantation and desorption, H_2 molecules formed locally in carbon are not distinguishable form the ones possibly originating from H–H mo-

lecular recombination in the chamber. Therefore, the difference between the H_2 signal and the actual H depletion should be smaller. This is not observed. On the contrary, similar or even larger differences are observed, in disagreement with the assumption of Ref. [7].

In a review paper, Causey [1] reports experiments [20–23] where different types of graphite where exposed to low energy deuterium during several hours at temperatures ranging from 323 to 1023 K. In some cases, deuterium was found at up to ∼1 mm depth; but it should be mentioned that some of these graphites showed significant porosity. The carbon material used in our study shows low porosity, but far in-depth transport of the molecules could be responsible for the measured H_2 deficit. In the next section, we will examine in more details the depth profile modification and try to find an explanation for this phenomenon.

4.3. Depth profile modification

As mentioned above, the H or D depth profile modifications were measured after single laser flashes. It is worth to mention that the initial profile is each time the implanted profile. Depth profiles obtained after single laser shots of different energy densities should not be interpreted as a sequence of depth profiles. The depth profiles obtained at lower energy density are not intermediate stages of depth profiles obtained at higher energy densities. The temperature increases quickly to its maximum, so the hydrogen can behave in a different manner. Also, laser flashes of higher energy densities keep the sample temperature high for a longer time.

Fig. 2 points out that the depletion is proportionally smaller for the lower concentration sample. This fact is compatible with the local molecular recombination model, i.e. 2nd order kinetics [2]. In this model, the particles form H_2 molecules at a rate proportional to the local concentration $C(x)$ and those molecules desorb to the surface. However, it is seen in Fig. 2(a) that the loss is preferential in the deeper part of the depth profile, after a 1.5×10^4 J/m² laser flash. The same is observed in Fig. 2(b) and (c) for the highest energy shot (1.7×10^4 J/m²), while no such effect is seen after the lower energy laser flash (1.1×10^4 J/m²). Similar results were also obtained at higher implantation energy and higher dose, as seen in Fig. 3(a). The highest energy density (1.3×10^4 J/m²) even induces retrapping near the surface. This could be explained by considering that at high temperature (>1700 K), molecular H is relatively less stable, with respect to atomic H. Indeed it is well known that H_2 can be dissociated by hot filaments in a vacuum chamber; it is conceivable that this is also true inside graphite and would explain both atomic re-emission at high T and H atom retrapping once the sample cools down after the laser flash. Atomic H also diffuses more rapidly at such temperature.

One must therefore consider that the hydrogen is still trapped (or even retrapped) in some stronger trap sites, such as the vacancy profile created during the implantation. This vacancy profile, calculated for 1.5 keV H by means of the computer code TRIM95 [24], also appears in Fig. 3(a). Because the mean range calculated by TRIM95 is 1/3 smaller compared to the measured one [12], the depth scale of the vacancy profile was multiplied by 1.5 in order to account for this discrepancy. The vacancy profile has quite the same shape as the peak of the depth profile obtained after the 1.3×10^4 J/m² laser flash. The lost fraction profile (Fig. 3(b)) shows that for the 0.7 and 0.9×10^4 J/m² laser shots, almost no desorption occurs in the first 15×10^{20} C/m² of depth, while strong retrapping is observed in the same range after the 1.3×10^4 J/m² shot.

The effect is stronger with increasing initial concentration, because more vacancies are created during the implantation. A sample implanted at lower concentration (Fig. 4(a)) retained an equal H fraction (41%) after a laser flash of similar energy (1.2×10^4 J/m²), but no comparable H accumulation is seen in the vacancies. Nevertheless, after a laser flash of high energy density (1.7×10^4 J/m²), this sample still features a maximum in the vacancy profile region. On the other hand, no such accumulation in the vacancy profile is observed for the deuterium implanted in HOPG, as seen in Fig. 4(b) (although we admit that the sensitivity of the ERD technique is worse for D compared to H). Most of the deuterium was desorbed after a 1.9×10^4 J/m² laser flash. This suggests that the hydrogen which fills the vacancies in experiments with H implantation could come mainly from the intrinsic H in the material. This is confirmed by the H depth profile in Fig. 4(b), which was obtained from the same 1.9×10^4 J/m² laser spot on the D implanted sample.

These results can be compared to those of Sawicki et al. [5] who implanted 30 keV T in polycrystalline graphite (5890/PT) and measured the depth profile modification. The depth profile extended in depth between 0.2 and 0.7 μm essentially. No significant shift in mean depth or change in distribution width were observed during a thermal desorption process reaching up to 1575 K. No measurement of the desorbing molecules was made. However, the T concentration was low (<0.5%) with, consequently, low damage creation. Besides, the vacancy profile increases quite gradually from the surface to the implantation mean range at 30 keV, according to TRIM95 simulation. Hence, it was not possible in this case to observe any preferential trapping or retrapping in these sites.

Some depth profile modifications were also obtained for an other type of carbon material, the vitreous carbon. The Fig. 1 showed the same discrepancy between the released H_2 and the desorbed H as measured by ERD-$E \times B$. According to the depth profile measure-

ments (Fig. 5), the H is already significantly depleted from the v-C at a relatively low temperature $(0.13 \times 10^4 \ J/m^2 = 840 \ K)$. Such low temperature desorption could indicate that the trapping energy is smaller than 0.6 eV, as evaluated from the H_2 signal. Once again, it is seen from the desorbed fraction profiles in Fig. 5(b) that the desorption is clearly preferential in the deeper part of the depth profile. The H peak corresponds also to the vacancy profile plotted in Fig. 3(a), which is closer to the surface compared to the depth profile. However, when the temperature reaches ~1500 K, most of the H contained in this part of the depth profile desorbs.

5. Conclusion

Laser induced desorption experiments were conducted on carbon materials of different types implanted with low energy hydrogen and deuterium. A comparison between the amount of hydrogen released as H_2 molecules and the actual retained quantity measured by means of ERD-$E \times B$ confirms that a large amount of hydrogen is effectively released from the implantation zone otherwise than by molecular recombination followed by desorption to the surface. Atomic H re-emission or far in-depth transport of the molecules could be some of the processes responsible for the disparity. For the vitreous carbon, a significant H amount is desorbed by these alternative processes at low temperature.

It is seen from the depth profile modification that at low laser energy density (i.e. low temperature), the modification is roughly compatible with a local molecular recombination model, without observable limitation by diffusion. At higher energy density corresponding to temperatures around 1700 K, while a broadening of the depth profile is not observed (as one expects from a diffusion process), a significant proportion of hydrogen is trapped in the vacancy profile, which would involve some relatively short range atomic diffusion.

Acknowledgements

References

[1] R.A. Causey, J. Nucl. Mater. 162 (1989) 151.
[2] K.L. Wilson, R.A. Causey, W.L. Hsu, B.E. Mills, M.F. Smith, J.B. Withley, J. Vac. Sci. Technol. A 8 (3) (1988) 1750.
[3] J. Roth, J. Bohdansky, K.L. Wilson, J. Nucl. Mater. 111 (1982) 775.
[4] K. Ashida, K. Watanabe, J. Nucl. Mater. 183 (1991) 89.
[5] J.A. Sawicki, J. Roth, L.M. Howe, J. Nucl. Mater. 162 (1989) 1019.
[6] H.Y. Guo, G.G. Ross, B. Terreault, J. Vac. Sci. Technol. A 10 (1992) 368.
[7] D. Kéroack, B. Terreault, J. Nucl. Mater. 231 (1996) 47.
[8] G.G. Ross, B. Terreault, C. Boucher, R. Boivin, J. Vac. Sci. Technol. A 4 (1986) 1243.
[9] R. Boivin, G.G. Ross, B. Terreault, J. Appl. Phys. 73 (1993) 1936.
[10] B. Terreault, J. Appl. Phys. 62 (1987) 152.
[11] J. L'Écuyer, C. Brassard, C. Cardinal, J. Chabbal, L. Deschênes, J.P. Labrie, B. Terreault, J.G. Martel, R. St-Jacques, J. Appl. Phys. 47 (1976) 381.
[12] G.G. Ross, L. Leblanc, Nucl. Instrum. Meth. B 83 (1993) 15.
[13] F. Schiettekatte, A. Chevarier, N. Chevarier, A. Plantier, G.G. Ross, Nucl. Instrum. Meth. B 118 (1996) 307.
[14] F. Schiettekatte, G.G. Ross, A. Chevarier, N. Chevarier, A. Plantier, Nucl. Instrum. Meth. B 132 (1997) 607.
[15] F. Schiettekatte, G.G. Ross, in: Proceedings of the 14th International Conference on the Application of Accelerators in Research and Industry, AIP, 1996, CP 392, 1997, p. 711.
[16] B. Terreault, D. Kéroack, G.G. Ross, R.G. St-Jacques, F. Schiettekatte, K. Touhouche, P. Zheng, J. Nucl. Mater. 220 (1995) 790.
[17] P. Franzen, E. Vietzke, A.A. Haasz, J.W. Davis, V. Phillips, J. Nucl. Mater. 196 (1992) 967.
[18] P. Franzen, E. Vietzke, J. Vac. Sci. Technol. A 12 (1994) 820.
[19] J.W. Davis, A.A. Haasz, J. Nucl. Mater. 220 (1995) 832.
[20] P.C. Stangeby, O. Auciello, A.A. Haasz, B.L. Doyle, J. Nucl. Mater. 122 (1984) 1592.
[21] R.A. Causey, K.L. Wilson, J. Nucl. Mater. 138 (1986) 57.
[22] R.A. Causey, M.I. Baskes, K.L. Wilson, J. Vac. Sci. Technol. A 4 (1986) 1189.
[23] R.A. Strehlow, J. Vac. Sci. Technol. A 4 (1986) 1183.
[24] J.F. Ziegler, J.P. Biersack, The Stopping and Range of Ions in Solids, Pergamon, New York, 1985.